

Dynamics of a Four-Dimensional Economic Model

Gheorghe Moza ^{1,*} , Oana Brandibur ²  and Ariana Găină ² ¹ Department of Mathematics, Politehnica University of Timisoara, 300006 Timisoara, Romania² Department of Mathematics, West University of Timisoara, 300223 Timisoara, Romania

* Correspondence: gheorghe.moza@upt.ro

Abstract: The interdependency between interest rates, investment demands and inflation rates in a given economy has a continuous dynamics. We propose a four-dimensional model which describes these interactions by imposing a control law on the interest rate. By a qualitative analysis based on tools from dynamical systems theory, we obtain in the new model that the three economic indicators can be stabilized to three equilibrium states.

Keywords: dynamical systems; bifurcation diagrams; economic models; local dynamics

MSC: 37G10; 34C23; 37N40

1. Introduction

Many economic and financial phenomena are modeled by dynamical systems based on differential or difference Equations [1–5]. Financial exhibition can be seen as an elective, flexible and active inquiry field that can be used to modify the functions of any investigation method, strategy or inquiry center. According to [6], financial demonstration may be thought as a multi-discipline research strategy that encourages the consideration of a variety of socio-economic-political concerns which can have a negative impact on society anywhere and at any time. However, it shall be asserted that financial demonstration has become an essential technical-theoretical explanatory instrument for future academics, financial experts, strategy builders and transnational educators. The importance of “stabilizing an unsteady economy” through adequate macroeconomic stabilization measures implemented by government and central bank is highlighted. It is vital to understand how business emergencies arise and how they can be managed in order to be proficient in these tactics. As a result, studying dynamic nonlinear macroeconomic models could provide new insights in this area.

Various models and methods for examining economic indicators of an economy can be found in the literature. Modeling principles in economic environments is presented in [7]. A book dealing with economic models based on ordinary and partially differential equations is [8], where the following three topics of financial engineering are covered: control and stabilization in financial models, state estimation and forecasting and validation by statistical methods of decision-making tools. A macroeconomic model applied to three national economies is presented in [9], where approach is based on three main tools: the state-space modeling from control theory, fractional calculus and orthogonal distance fitting method. A model for studying the perspective of annual flow of inheritance (in level or as a share of national income) in a two-sector economy with one pure consumption good and one capital good was recently presented in [10]. Using tools from dynamical systems theory, two endogenous behaviors, which can operate independently or together, are obtained. It is shown that theoretical results provided by the model are consistent with some empirical data. In a recent paper [11], a deep learning method for matching the production of wind energy with consumers’ needs is presented. A neural ordinary differential equation is used to model the wind speed continuously. A mathematical model based on differential



Citation: Moza, G.; Brandibur, O.; Găină, A. Dynamics of a Four-Dimensional Economic Model. *Mathematics* **2023**, *11*, 797. <https://doi.org/10.3390/math11040797>

Academic Editor: Huaizhong Zhao

Received: 20 December 2022

Revised: 1 February 2023

Accepted: 1 February 2023

Published: 4 February 2023



Copyright: © 2023 by the authors. Licensee MDPI, Basel, Switzerland. This article is an open access article distributed under the terms and conditions of the Creative Commons Attribution (CC BY) license (<https://creativecommons.org/licenses/by/4.0/>).

equations for studying epidemic and economic consequences of COVID-19 is presented in [12]. The model deals mainly with interactions between the disease transmission, the pandemic management, and the economic growth. A macroeconomic development model, known as the Grossman–Helpman model of endogenous product cycles, is presented in [13], where the stabilization problem is studied by a method based on optimal control.

A three-dimensional (3D) model to study the interactions of three macroeconomic indicators in a given economy is presented in [14]. This model is based on three ordinary differential equations and was designed to describe the relationships between three financial instruments: the interest rate $x(t)$, the investment demand $y(t)$ and the inflation rate $z(t)$. By studying the local behavior of the model around one of its equilibrium points, conditions to stabilize the economy around this steady state have been obtained in [14]. The finance system is an essential component of our economy that consist of interactions between the institutional units and markets, generally in a complex manner for the purpose of economic growth in investment and the demand of commercials. When an inflation occurs and a chaotic phenomenon appears in the finance system, the interest rate must be adjusted and controlled, regarding our model, it is possible by introducing a control function. The control of finance system goes to a quick and effective revival of the economy. This method is used when an economic crisis occurs. In order to find more economically relevant steady states to which the 3D model could be stabilized, we apply a control function to the model and study the resulting four-dimensional (4D) system. In addition, we consider in this work that $x(t)$ is the *real* interest rate, which is defined as the difference between the nominal interest rate and the inflation rate, thus, $x(t)$ may take positive or negative values.

A generalization to fractional order version of the 3D model is reported in [15], while in [16] the generalized model is studied in a new framework with delay. Moreover, Ref. [16] investigates by numerical simulations the effect of time delay to chaos in the model, while methods to suppress chaos in the model were presented in [17]. Fractional-order dynamical models and their bifurcations [18–23] are promising tools for studying economic models.

The paper is organized as follows: after the introduction, Section 2 describes the model to be studied and presents a local analysis of its behavior, where equilibrium points are characterized in terms of their type and stability properties. The occurrence of transcritical and pitchfork bifurcations when the system’s parameters vary is particularly pointed out. Section 3 provides bifurcation diagrams for several combinations of parameters, revealing the complex behavior of the system.

2. Local Analysis of the Model

The 3D system studied in [14] is given by

$$\dot{x} = z + x(y - a), \dot{y} = -x^2 - by + 1, \dot{z} = -x - cz, \tag{1}$$

where $\dot{x} = \frac{dx}{dt}$ denotes the usual derivative with respect to time. The system has been studied in the first octant given by $x \geq 0, y \geq 0$ and $z \geq 0$, where $x = x(t)$ is the real interest rate, $y = y(t)$ the investment demand, $z = z(t)$ the inflation rate, $a \in \mathbb{R}$ the amount (of money) saved, $b \geq 0$ the cost per investment, $c > 0$ the elasticity of the demand on the commercial market.

We propose in this work to apply a feedback control function $u(t)$ to the first equation of (1) in the form

$$\dot{x}(t) = z(t) + x(t)(y(t) - a) - u(t), \tag{2}$$

where $u(t) = u(0)e^{\int_0^t (m-dx(t))dt}$, with $m, d \in \mathbb{R}$ and $d \neq 0$. Then, u satisfies the equation $\dot{u} = u(m - dx)$, which, together with (2), lead to a new four-dimensional (4D) system, given by

$$\dot{X} = F(X, \mu), \tag{3}$$

where $X = (x \ y \ z \ u)^T, F(X, \mu) = (f_1 \ f_2 \ f_3 \ f_4)^T$, respectively,

$$f_1 = z + x(y - a) - u, f_2 = -x^2 - by + 1, f_3 = -x - cz \text{ and } f_4 = u(m - dx).$$

The parameter vector is $\mu = (a, b, c, d, m)$; T stands for the transpose here.

Therefore, the four-dimensional system of differential equations to be studied is

$$\begin{cases} \dot{x} = z + x(y - a) - u \\ \dot{y} = -x^2 - by + 1 \\ \dot{z} = -x - cz \\ \dot{u} = u(m - dx) \end{cases}.$$

The model (3) presents economic relevance whenever its state variables lie in the set

$$\Sigma = \{(x, y, z, u) | x \in \mathbb{R}, y \geq 0, z \geq 0, u \in \mathbb{R}\}.$$

The new differential equation in $\dot{u}(t)$ leads in general to a different behavior of all state variables in the 4D model compared to the 3D model. In what follows, a qualitative analysis of the new model is investigated by well-known tools from the dynamical systems theory, providing several bifurcation diagrams which describe the local dynamics of the model around its equilibrium points.

The control introduced in this work by (2) is far from being unique. More other different control laws can be proposed. They can be designed as equations of type (2) or other types of constraints applied to one or more of the basis equations of the model. Their final role is to determine different behaviors of the transformed 3D model, which have economic relevance and are desirable in an economy.

Remark 1. The hyperplane $u = 0$ is invariant with respect to the flow of (3). The model (3) with $u = 0$ and $x(t) \geq 0$ was studied in [14].

Our next step is to determine the equilibrium points (x^*, y^*, z^*, u^*) of system (3), which are the solutions of the algebraic system

$$\begin{cases} z + x(y - a) - u = 0 \\ -x^2 - by + 1 = 0 \\ -x - cz = 0 \\ u(m - dx) = 0 \end{cases}.$$

The system (3) has four isolated equilibrium points: $P_1 = (0, \frac{1}{b}, 0, 0)$ for all $a, m \in \mathbb{R}$, $b > 0, c > 0$ and $d \neq 0$, the pair $P_2 = (\sqrt{\alpha}, \frac{ac+1}{c}, -\frac{1}{c}\sqrt{\alpha}, 0)$ and $P_3 = (-\sqrt{\alpha}, \frac{ac+1}{c}, \frac{1}{c}\sqrt{\alpha}, 0)$ for all $a, m \in \mathbb{R}, b \geq 0, c > 0, d \neq 0$ and $\alpha = \frac{1}{c}(c - b - abc) \geq 0$, respectively, $P_4 = (x_4, \frac{1-x_4^2}{b}, -\frac{x_4}{c}, x_4 \frac{c-b-cx_4^2-abc}{bc})$, where $x_4 = \frac{m}{d}$, for all $a, m \in \mathbb{R}, b > 0, c > 0$ and $d \neq 0$.

Remark 2. Since $x(t)$ may be positive or negative in (3), three different equilibrium points (P_1, P_3 and P_4) with economic relevance arise in the 4D model (3), while in the 3D model (1) only one equilibrium presented economic relevance and was studied in [14]. Notice that P_4 coincides with P_1 if $m = 0$, respectively, P_2 and P_3 collide to P_1 on $\alpha = 0$ and $b > 0$.

In addition, the system has two more non-isolated equilibria for $b = 0$, that is, $Q_y = (1, y, -\frac{1}{c}, y - a - \frac{1}{c})$ if $m = d \neq 0$, respectively, $S_y = (-1, y, \frac{1}{c}, -y + a + \frac{1}{c})$ if $m = -d \neq 0$.

If P is a saddle equilibrium point, denote by (n_s, n_u) the dimensions of its stable and unstable manifolds. For $b > 0$, denote by $\beta_1 = \frac{1}{2b}(1 - ab - bc)$.

Theorem 1. Assume $m > 0$. Then:

- (a) if $\alpha > 0$, the equilibrium point P_1 is a saddle with $(n_s, n_u) = (2, 2)$;
- (b) if $\alpha < 0$ and $\beta_1 < 0$, the equilibrium point P_1 is a saddle with $(n_s, n_u) = (3, 1)$;
- (c) if $\alpha < 0$ and $\beta_1 > 0$, the equilibrium point P_1 is a saddle with $(n_s, n_u) = (1, 3)$.

The next result gives us a characterization of the nature of the equilibrium point P_1 for the case when the parameter m involved in the differential equation of system (3) describing the control function u is negative. Moreover, the dimensions of the stable and unstable manifolds are established, respectively.

Theorem 2. Assume $m < 0$. Then,

- (a) P_1 is a saddle with $(n_s, n_u) = (3, 1)$ if $\alpha > 0$, respectively, $(n_s, n_u) = (2, 2)$ if $\alpha < 0$ and $\beta_1 > 0$;
- (b) P_1 is an attractor whenever $\alpha < 0$ and $\beta_1 < 0$;
- (c) if $0 < c < 1$, a Hopf bifurcation occurs at P_1 on $(H) : 1 - ab - bc = 0$.

Proof. The eigenvalues associated with the equilibrium point P_1 are $-b, m$ and $\lambda_{p_1}^\pm = \beta_1 \pm \sqrt{\Delta_1}$, where $\beta_1 = \frac{1}{2b}(1 - ab - bc)$ and $\Delta_1 = \frac{(1-ab+bc)^2}{4b^2} - 1$. Since $\lambda_{p_1}^+ \lambda_{p_1}^- = -\frac{c-b-abc}{b}$ and $\lambda_{p_1}^+ + \lambda_{p_1}^- = \frac{1-ab-bc}{b}$, the proofs of the above theorems follow (except the point c) of the last theorem.

For the case (c), assume β_1 is the bifurcation parameter. A necessary condition to have Hopf bifurcation at P_1 is $\Delta_1 < 0$, which is equivalent to $-(1 + c) < \beta_1 < 1 - c$. It follows that β_1 can cross 0 from negative to positive values if and only if $0 < c < 1$. At $\beta_1 = 0$ the obtained eigenvalues $\pm i\sqrt{1 - c^2}$ are purely complex. Since $\left. \frac{\partial(\text{Re}(\lambda_{p_1}^\pm))}{\partial\beta_1} \right|_{\beta_1=0} = 1$ if $\Delta_1 < 0$, a Hopf bifurcation occurs on H . The bifurcation is non-degenerate if the first Lyapunov coefficient $l_1(0)$ is nonzero, in which case a limit cycle (stable or unstable) arises around the equilibrium P_1 when β_1 crosses 0. If $l_1(0) = 0$, the bifurcation becomes degenerate and more limit cycles may arise around P_1 when β_1 crosses 0. \square

In the following we study how the equilibrium point P_4 bifurcates from the equilibrium point P_1 when the parameter m crosses 0, respectively, how equilibrium points P_2 and P_3 are born from P_1 when parameter α increases from 0. We will show that the equilibrium points bifurcate from P_1 through transcritical, respectively, pitchfork bifurcations.

Theorem 3. Assume $b > 0$. The system undergoes a transcritical bifurcation at $m = 0$ if $\alpha \neq 0$ and $\beta_1 \neq 0$, respectively, a pitchfork bifurcation at $\alpha = 0$ if $m \neq 0$ and $c \neq \pm 1$.

Proof. If $m = 0, \alpha \neq 0$ and $\beta_1 \neq 0$, the eigenvalues of P_1 are $-b, 0$ and $\lambda_{p_1}^\pm$, with $\text{Re}(\lambda_{p_1}^\pm) \neq 0$; if $\lambda_{p_1}^\pm$ are real, this follows from $\lambda_{p_1}^+ \lambda_{p_1}^- = -\frac{\alpha c}{b} \neq 0$. To prove the transcritical bifurcation, we will use Sotomayor’s theorem [23]. Denote by $\mu_0 = (a, b, c, d, 0)$. The Jacobian matrix $J_0 = DF(P_1, \mu_0)$ of the vector field F , expressed at P_1 and $\mu = \mu_0$, has an eigenvalue $\lambda = 0$ with a corresponding eigenvector $v = (-bc \ 0 \ b \ -c\alpha)^T$. The value $\lambda = 0$ is also an eigenvalue for the transpose matrix J_0^T , which has a corresponding eigenvector $w = (0 \ 0 \ 0 \ 1)^T$; T stands for the transpose here.

It is clear that $w^T \cdot F_m(P_1, \mu_0) = 0$ and $w^T \cdot [DF_m(P_1, \mu_0) \cdot v] = -c\alpha \neq 0$, where $F_m = \frac{\partial F}{\partial m} = (0 \ 0 \ 0 \ u)^T$; DF_m is the Jacobian matrix of the vector field F_m . It remains to determine $D^2F(P_1, \mu_0)(v, v)$, where, by definition $D^2F = (d^2f_1 \ d^2f_2 \ d^2f_3 \ d^2f_4)^T$. For a real-valued function $f : V \subset \mathbb{R}^4 \rightarrow \mathbb{R}, x \mapsto f(x), x = (x_1, x_2, x_3, x_4), V$ open, and a vector $v = (v_1, v_2, v_3, v_4), d^2f(v, v) = \sum_{i,j=1}^4 \frac{\partial^2 f}{\partial x_i \partial x_j} v_i v_j$ denotes the differential of second order

applied to the pair (v, v) . Taking into account the expression of w , one needs to determine only $d^2f_4(v, v)$ at (P_1, μ_0) , which is $-2dv_1v_4 = -2bc^2d\alpha$. Finally, $w^T \cdot [D^2F(P_1, \mu_0)(v, v)] = -2bc^2d\alpha \neq 0$.

For the pitchfork bifurcation at $\alpha = 0$, we observe first that $\Sigma := \{u = 0\}$ is an invariant manifold of the system (3). Since $P_{2,3} \in \Sigma$ for all $\alpha \geq 0$, the bifurcation takes place on Σ and can be studied by restricting the system (3) to Σ . Translating first P_1 to the origin $O(0, 0, 0)$ by $y \rightarrow y - \frac{1}{b}$, the system (3) restricted to Σ reads

$$\dot{Y} = G(Y, \mu), \tag{4}$$

where $Y = (x \ y \ z)^T, G(Y, \mu) = (g_1 \ g_2 \ g_3)^T$, respectively,

$$g_1 = z + x(y - a + 1/b), \ g_2 = -x^2 - by \text{ and } \ g_3 = -x - cz.$$

$P'_2 = (-\sqrt{\alpha}, \frac{ac+1}{c} - \frac{1}{b}, \frac{1}{c}\sqrt{\alpha})$ and $P'_3 = (\sqrt{\alpha}, \frac{ac+1}{c} - \frac{1}{b}, -\frac{1}{c}\sqrt{\alpha})$, $a \in \mathbb{R}, b > 0, c > 0$ and $\alpha = \frac{1}{c}(c - b - abc) \geq 0$, become equilibrium points of the system (4).

The stability of the equilibrium O in the system (4) has been studied in [14]. In addition to the results from [14], we show that the points P'_2 and P'_3 are born from O when α crosses 0 from negative to positive values by a bifurcation of type nondegenerate pitchfork. This bifurcation was not studied in [14].

Consider α the bifurcation parameter with $m \neq 0$ and $c \neq \pm 1$. P'_2 and P'_3 collide to O at $\alpha = 0$. The eigenvalues of O in (4) at $\alpha = 0$ are $0, -b$ and $\frac{1}{c} - c$, with the corresponding eigenvector to 0 given by $v = (-c \ 0 \ 1)^T$.

The system (4) is \mathbb{Z}_2 -equivariant with the symmetry $R(Y) = (-x \ y \ -z)^T$. Indeed, $R(R(Y)) = Y$ and $R \circ G(Y, \mu) = G \circ R(Y, \mu)$. In other words, the system (4) remains unchanged by applying the transformation $(x, y, z) \xrightarrow{R} (-x, y, -z)$. Notice that, we can write $\mathbb{R}^3 = X^+ \oplus X^-$, where $X^+ = \{(0, y, 0), y \in \mathbb{R}\}$ and $X^- = \{(x, 0, z), x, z \in \mathbb{R}\}$, such that $R(Y) = Y$ if $Y \in X^+$ and $R(Y) = -Y$ if $Y \in X^-$. With these notations, it follows that $v \in X^-$; when needed, we write a vector $(x \ y \ z)^T$ as (x, y, z) .

Thus, applying a result from [24] page 284, the system (4) undergoes a pitchfork bifurcation at $\alpha = 0$, which can be degenerate or not. To determine which is the case, we proceed as it follows. Find first the normal form of (4). To this end, consider the transformation $Z = P^{-1}Y$, where $P = (v_1 \ v_2 \ v_3)$ is a column matrix containing the eigenvectors corresponding to the eigenvalues $0, -b$ and $\frac{1}{c} - c$ of O at $\alpha = 0$, that is, $v_1 = (-c \ 0 \ 1)^T, v_2 = (0 \ 1 \ 0)^T$ and $v_3 = (-1 \ 0 \ c)^T$, and $Z = (z_1 \ z_2 \ z_3)^T$. The system (4) in the new variables z_1, z_2 and z_3 reads

$$\dot{z}_1 = k(z_3 + cz_1)z_2, \ \dot{z}_2 = -bz_2 - c^2z_1^2 - 2cz_1z_3 - z_3^2, \ \dot{z}_3 = -\frac{1}{k}z_3 - kz_1z_2 - \frac{k}{c}z_2z_3, \tag{5}$$

where $k = \frac{c}{c^2-1}$. Since the eigenvalues of O in (4) at $\alpha = 0$ are $0, -b$ and $\frac{1}{c} - c$ (in this order), we consider the extended system of dimension 4 formed by $\dot{\alpha} = 0$ and the three equations from (5). The new system has at $\alpha = 0$ the eigenvalues $0, 0, -b$ and $\frac{1}{c} - c$, thus, applying the Center Manifold Theorem, there exists a two-dimensional center manifold W_c^α of class C^∞ of the form $z_2 = h_2(z_1, \alpha)$ and $z_3 = h_3(z_1, \alpha), h_2, h_3 \in C^\infty$, which locally (in cubic terms) can be expressed by

$$z_2 = \sum_{i+j \leq 3} c_{ij}z_1^i \alpha^j \text{ and } z_3 = \sum_{i+j \leq 3} d_{ij}z_1^i \alpha^j.$$

Using the method of undetermined coefficients, we found $c_{20} = \frac{-c^2}{b}, d_{30} = \frac{c^4}{b(c^2-1)^2}$, while the other coefficients are all 0. Therefore, the system (5) on the center manifold W_c^α is of the form

$$\dot{z}_1 = \beta(\alpha)z_1 + \sigma_0z_1^3 + \dots$$

where $\beta(\alpha)$ is a smooth function of α with $\beta(0) = 0$ and $\sigma_0 = \frac{c^4}{b(1-c^2)} \neq 0$, thus, the pitchfork bifurcation is non-degenerate. To find the function $\beta(\alpha)$, higher order terms are needed in the expressions of $h_2(z_1, \alpha)$ and $h_3(z_1, \alpha)$.

We notice that the coefficient σ_0 could be obtained without considering the extended system, by finding the 1-dimensional center manifold W_c directly in the system (5) and then the restriction of (5) on W_c . In this case, W_c is given locally by $z_2 = \sum_{i=1}^3 c_i z_1^i$ and $z_3 = \sum_{i=1}^3 d_i z_1^i$. Applying the method of undetermined coefficients, one can show $c_2 = -\frac{c^2}{b}$ and $d_3 = \frac{1}{b} \frac{c^4}{(c^2-1)^2}$, while the other coefficients are 0. These lead to $\dot{z}_1 = \sigma_0 z_1^3 + \dots$. The advantage of using the extended system is that $\beta(\alpha)$ may also be determined. \square

Remark 3. The Sotomayor’s theorem for pitchfork bifurcation gives no answer to the problem because $D^3F = (0 \ 0 \ 0 \ 0)^T$.

The local behavior of the system (3) at $P_{2,3}$. The characteristic polynomial at P_2 and P_3 with $\alpha > 0$ is $P(\lambda) = (\lambda - m \pm d\sqrt{\alpha})Q(\lambda)$, where

$$Q(\lambda) = \lambda^3 + s_2\lambda^2 + s_1\lambda + 2c\alpha,$$

$s_2 = \frac{1}{c}(c^2 + bc - 1)$ and $s_1 = \frac{1}{c}(bc^2 + 2c\alpha - b)$; “+” corresponds to P_2 and “-” to P_3 . Denote by λ_1, λ_2 and λ_3 the roots of $Q(\lambda)$, respectively, $\lambda_4^{P_2} = m - d\sqrt{\alpha}$ and $\lambda_4^{P_3} = m + d\sqrt{\alpha}$. Since the roots of $Q(\lambda)$ satisfy $\lambda_1\lambda_2\lambda_3 < 0$, $P_{2,3}$ are saddles or attractors. Denote by $s_3 = s_2s_1 - 2c\alpha$. By Routh–Hurwitz conditions, λ_1, λ_2 and λ_3 have negative real parts if and only if

$$s_2 > 0 \text{ and } s_3 > 0, \tag{6}$$

which are equivalent to $c(b + c) > 1$ and $b(1 - bc)(2ac + 3) + bc^3(b + c) - 2c > 0$. We notice that (6) are satisfied at least for $\alpha > 0$ sufficiently small and $c^2 > 1$. The results are summarized in the next Theorem 4. The attractors P_2 and P_3 with orbits converging to them are illustrated in Figure 1.

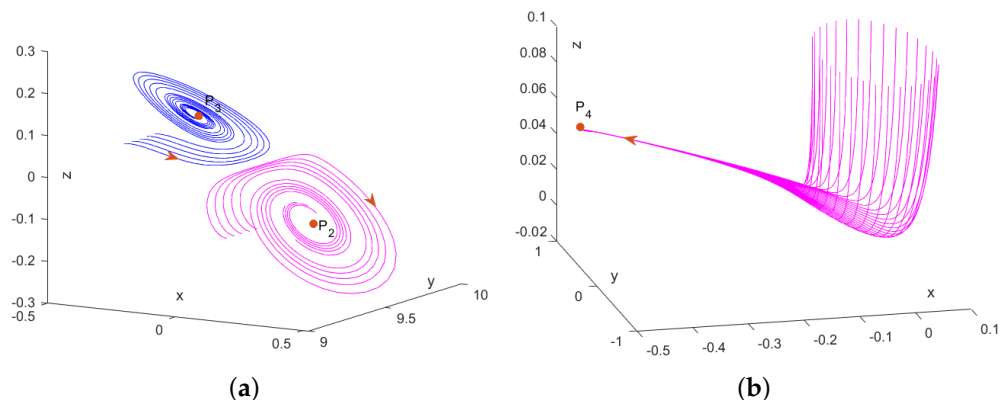


Figure 1. (a) Orbits around the attractors P_2 and P_3 in the system (3) projected in the xyz space. The parameters are $a = 9, b = 0.1, c = 2, m = d = -1$. The starting points for P_2 are $(0.2, 9 + i/2, -0.1, 0.05)$, while for P_3 they are $(-0.2, 9 + i/2, 0.1, 0.05)$, for $i = 0, 1, 2, 3, 4$. (b) Orbits around the attractor P_4 for $a = b = 1, c = 10, m = 0.1$ and $d = -0.2$.

Theorem 4. Assume $\alpha > 0$. Then, P_2 and P_3 are attractors if (6) is satisfied and $\lambda_4^{P_2} < 0$ for P_2 , respectively, $\lambda_4^{P_3} < 0$ for P_3 . In the other cases with $\lambda_4^{P_{2,3}} \neq 0$, P_2 and P_3 are saddles.

The local behavior of the system (3) at P_4 . The characteristic polynomial at P_4 is

$$S(\lambda) = \lambda^4 + m_3\lambda^3 + m_2\lambda^2 + m_1\lambda + m_0,$$

where $m_3 = a + b + c - \frac{1}{b} + \frac{m^2}{bd^2}$, $m_2 = -\frac{c}{b}\alpha + \frac{m_0}{bc} + \frac{3b+c}{bd^2}m^2 - 2b\beta_1$, $m_1 = -c\frac{b+m}{b}\alpha + \frac{1}{c}m_0 + cm^2\frac{3b+m}{bd^2}$ and $m_0 = cm\frac{m^2-d^2\alpha}{d^2}$; $\alpha = \frac{1}{c}(c - b - abc)$ and $\beta_1 = \frac{1}{2b}(1 - ab - bc)$.

Remark 4. Denote by $\beta_2 = bc + bm + cm$ and $\beta_3 = b + c + m$. Then m_1 and m_2 can be written in the forms

$$m_1 = a\beta_2 + N_1 \text{ and } m_2 = a\beta_3 + N_2, \tag{7}$$

where $N_1 = m^2\frac{2bc+\beta_2}{bd^2} + (b - c)\frac{\beta_2}{bc}$ and $N_2 = m^2\frac{2b+\beta_3}{bd^2} + \frac{1}{bc}(b - c)m + \frac{c}{b}(b^2 - 1)$.

For $c > 0$ arbitrary fixed, define the following curves lying in the ba -parametric plane: $A = \{(b, a), \alpha = 0, b > 0\}$, $H = \{(b, a), \beta_1 = 0, b > 0\}$, $S_2 = \{(b, a), s_2 = 0, b > 0\}$, $S_3 = \{(b, a), s_3 = 0, b > 0\}$, $L_1 = \{(b, a), \lambda_4^{P_2} = 0, b > 0\}$, $L_2 = \{(b, a), \lambda_4^{P_3} = 0, b > 0\}$ and $M_i = \{(b, a), m_i = 0, b > 0\}$, $i = 1, 2, 3$. Notice that b corresponds to the x -axis, while a to the y -axis, and all curves are included in the region $b > 0$.

Theorem 5. If $m_0 < 0$, then P_4 is a saddle. Assume $m_0 > 0$. Then,

- (a) P_4 is a saddle or an attractor for all $d > 0$ and $m \neq 0$.
- (b) P_4 is an attractor if and only if $m_3 > 0$, $k_0 = m_3m_2 - m_1 > 0$ and $k_1 = (m_3m_2 - m_1)m_1 - m_3^2m_0 > 0$. In particular, if $\alpha < 0$, $\beta_1 < 0$, $b(b + c)(a + b) > c$ and $m > 0$ sufficiently small, P_4 is an attractor, as shown in Figure 1.

Proof. It is clear that P_4 is a saddle if $m_0 < 0$, since the product of its eigenvalues is negative.

- (a) Let further be $m_0 > 0$. Assume first $m > 0$, thus, $m^2 > \alpha d^2$. It is clear that $m_1 > 0$ if $\alpha \leq 0$, thus,

$$E_2 = \lambda_1\lambda_2(\lambda_3 + \lambda_4) + \lambda_2\lambda_3\lambda_4 = -m_1 < 0.$$

Let $\alpha > 0$. Then, $m^2 > \alpha d^2$ yields $m_1 > 2c\alpha + \frac{1}{c}m_0 > 0$, thus, $E_2 < 0$.

Secondly, assume $m < 0$. Then $m^2 < \alpha d^2$ and $\alpha > 0$ follow from $m_0 > 0$. For an arbitrary fixed $b > 0$, denote by $(b, a_{l_2}) \in L_2$, $(b, a_{m_1}) \in M_1$, $(b, a_{m_2}) \in M_2$ and $(b, a_{m_3}) \in M_3$ four points from the corresponding curves. Then,

$$a_{m_1} = -\frac{N_1}{\beta_2}, a_{m_2} = -\frac{N_2}{\beta_3}, a_{l_2} - a_{m_1} = \frac{2cm^2}{d^2\beta_2} \text{ and } a_{m_2} - a_{m_1} = N_3, \tag{8}$$

where $N_3 = (1 - c^2)\frac{b}{c\beta_3} + 2m^2\frac{c^2 - bm}{d^2\beta_2\beta_3}$. Notice that $a_{m_3} = \frac{1}{b} - c - b - \frac{m^2}{bd^2}$ and $a_{l_2} = \frac{1}{b} - \frac{1}{c} - \frac{m^2}{bd^2}$. More cases need to be considered further.

- (a1) Assume $\beta_2 \leq 0$. The curve L_2 is given by

$$a = a_{l_2}, \tag{9}$$

with $b > 0$ and $c > 0$. One can show that $m_0 > 0$ is equivalent to $a < a_{l_2}$. If $\beta_2 = 0$, then $m_1 = \frac{2b^2c^3}{d^2(b+c)^2} > 0$, thus, $E_2 = -m_1 < 0$. If $\beta_2 < 0$, then, from $m_1 = a\beta_2 + N_1$ and $a < a_{l_2}$, one gets $m_1 > \frac{2c}{d^2}m^2$, which leads to $E_2 < 0$.

- (a2) Assume $\beta_2 > 0$ and $0 < c \leq 1$. Then $\beta_3 > 0$ as well. Since $m_1|_{L_2} = \frac{2cm^2}{d^2} \neq 0$ and $m_2|_{M_1} = -N_3\beta_3 \neq 0$, it follows that $L_2 \cap M_1 = \emptyset$ and $M_2 \cap M_1 = \emptyset$; we denoted as usual by $m_1|_{L_2} = m_1(b, a)$ for $(b, a) \in L_2$. From (8), one get $a_{l_2} > a_{m_1}$ and $a_{m_2} > a_{m_1}$, since $N_3 > 0$ if $0 < c \leq 1$.

For $b > 0$, denote by $M_1^+ = \{(b, a), m_1 > 0, m_0 \geq 0\}$ and $M_1^- = \{(b, a), m_1 \leq 0, m_0 \geq 0\}$, the two regions from $m_0 \geq 0$ corresponding to $m_1 > 0$, respectively, $m_1 \leq 0$. Then $E_2 = -m_1 < 0$ on the region M_1^+ . Notice that $L_2 \subset M_1^+$, because $m_1|_{L_2} = \frac{2cm^2}{d^2} > 0$ and $L_2 \cap M_1 = \emptyset$.

If $m_1 \leq 0$, which is equivalent to $a \leq a_{m_1}$, one can show

$$m_2 \leq -N_3\beta_3 < 0,$$

whenever $0 < c \leq 1$. It follows that

$$E_3 = \lambda_1(\lambda_2 + \lambda_3 + \lambda_4) + \lambda_2(\lambda_3 + \lambda_4) + \lambda_3\lambda_4 = m_2 < 0,$$

on M_1^- . Therefore, $E_2 < 0$ or $E_3 < 0$ on $m_0 > 0$, whenever $\beta_2 > 0$ and $0 < c \leq 1$.

(a3) Assume $\beta_2 > 0$ and $c > 1$, thus, $\beta_3 > 0$. Since

$$m_1|_{L_2} = \frac{2cm^2}{d^2} \neq 0, m_2|_{L_2} > \frac{b}{c}(c^2 - 1) \neq 0 \text{ and } m_3|_{L_2} = b + c - \frac{1}{c} \neq 0,$$

it follows that $L_2 \cap M_1 = \emptyset, L_2 \cap M_2 = \emptyset$ and $L_2 \cap M_3 = \emptyset$. Notice that $a_{l_2} - a_{m_2} = \frac{bd^2(c^2-1)+2cm^2}{cd^2\beta_3} > 0$.

In the region $b > 0$, denote by $M_2^+ = \{(b, a), m_2 \geq 0, m_0 \geq 0\}$ and $M_2^- = \{(b, a), m_2 < 0, m_0 \geq 0\}$. Then $E_3 = m_2 < 0$ on the region M_2^- . Notice that $L_2 \subset M_2^+$, because $m_2|_{L_2} > \frac{b}{c}(c^2 - 1) > 0$ and $L_2 \cap M_2 = \emptyset$.

Assume further $m_2 \geq 0$. If $m_1 > 0$, then $E_2 = -m_1 < 0$. It remains the case $m_1 \leq 0$. We notice that M_2 may intersect M_1 in the region $m_0 \geq 0$, since

$$m_2|_{M_1} = 2m^2 \frac{bm - c^2}{d^2\beta_2} + \frac{b}{c}(c^2 - 1),$$

may be zero. The inequalities $m_2 \geq 0$ and $m_1 \leq 0$ yield $-\frac{N_2}{\beta_3} \leq a \leq -\frac{N_1}{\beta_2}$, thus, $N_2\beta_2 > N_1\beta_3$, which, in turns, leads to

$$\frac{m^2}{d^2} < \frac{\beta_2 b(c^2 - 1)}{2c(c^2 - bm)}. \tag{10}$$

Then, $-\frac{N_2}{\beta_3} \leq a$ and (10) yield

$$m_3 > \frac{-bcm(b + c) + c^2(c^2 - 1) + bc + mb}{c(c^2 - bm)},$$

which implies $m_3 > 0$, because $bc + mb > -mc > 0$ follows from $\beta_2 > 0$ and $m < 0$. Therefore,

$$E_4 = \lambda_1 + \lambda_2 + \lambda_3 + \lambda_4 = -m_3 < 0.$$

It follows that, $E_2 < 0$ or $E_3 < 0$ or $E_4 < 0$ whenever $m_0 > 0$, if $c > 0, d > 0$ and $m \neq 0$, which, in turn, imply that at least one eigenvalue λ_i has $Re(\lambda_i) < 0$. This confirms the proof.

(b) The result follows from Routh–Hurwitz conditions for $S(\lambda)$, which are $m_0 > 0, m_3 > 0, m_3m_2 > m_1$ and $k_1 > 0$. For the particular case, we write the expression k_1 as a polynomial in m ,

$$k_1(m) = \sum_{i=1}^8 c'_i m^i + \alpha\beta_1(b(b + c)(a + b) - c) \frac{2c}{b}$$

for some coefficients c'_i , thus, $k_1 > 0$. The condition $m_3m_2 > m_1$ follows from $k_1 > 0$ and $m_1 > 0$.

□

Example 1. The equilibrium point P_4 does not exist in the 3D model. This happens due to the control function $u(t)$, defined by the two constraints in the new 4D model. When P_4 is an attractor and $P_4 \in \Sigma$, the three state variables, namely the real interest rate $x = x(t)$, the investment demand $y = y(t)$ and the inflation rate $z = z(t)$, can be stabilized at least locally around three fixed values $\frac{m}{d}$, $\frac{d^2-m^2}{bd^2}$ and $-\frac{m}{cd}$, respectively, which are economically relevant if $md < 0$ and $d^2 > m^2$. This scenario does not arise in the 3D model since P_4 is not a steady state of the model.

3. Bifurcation Diagrams

Denote by R the region

$$R = \{(b, a), b \geq 0\}.$$

The curve A has a unique branch of the form $a = \frac{1}{b} - \frac{1}{c}$ lying in R , for all $c > 0$ arbitrary fixed, which splits the region R into two parts: $\alpha > 0$ in the region from R that contains the origin $(0, 0)$, and $\alpha < 0$ in the other region, as shown in Figures 2–5.

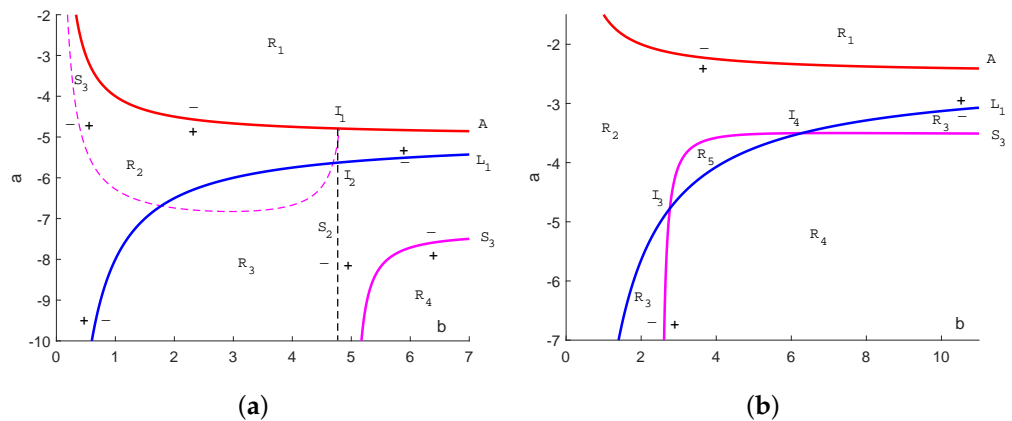


Figure 2. Bifurcation diagrams of the system (3) for $0 < c < 1$ and (a) $0 < m < c_0d$, respectively, (b) $m > c_0d > 0$, where $c_0 = \frac{c+1}{c}\sqrt{1-c^2}$.

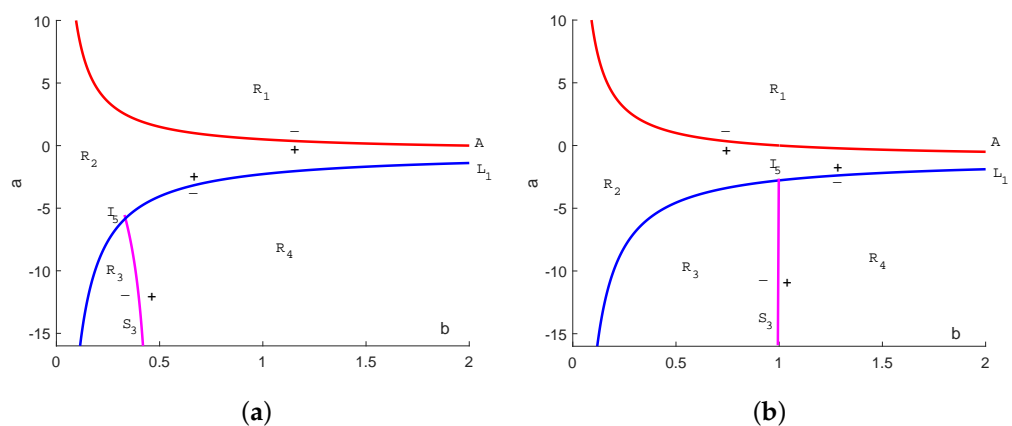


Figure 3. Bifurcation diagrams of the system (3) for $m > 0, d > 0$ and (a) $c > 1$, respectively, (b) $c = 1$.

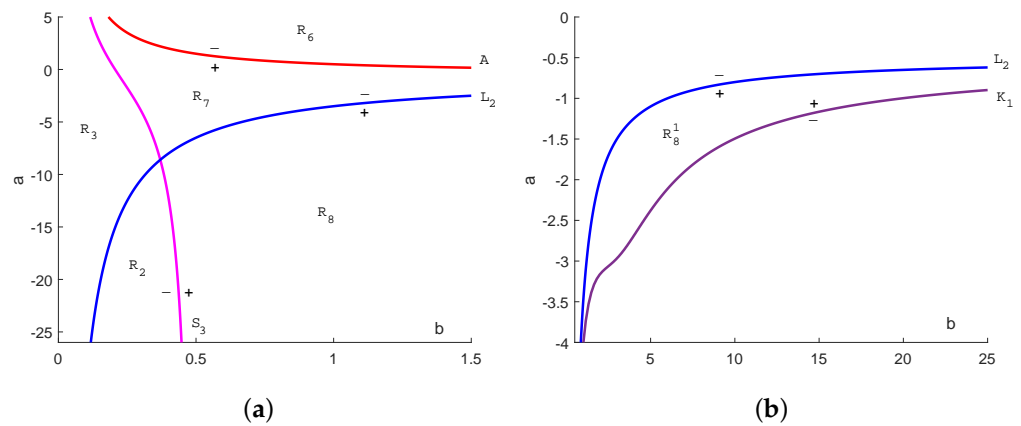


Figure 4. Bifurcation diagrams of the system (3) for $m < 0, d > 0$ and $c > 1$, (a,b). A region R_8^1 where P_4 is an attractor is presented in (b).

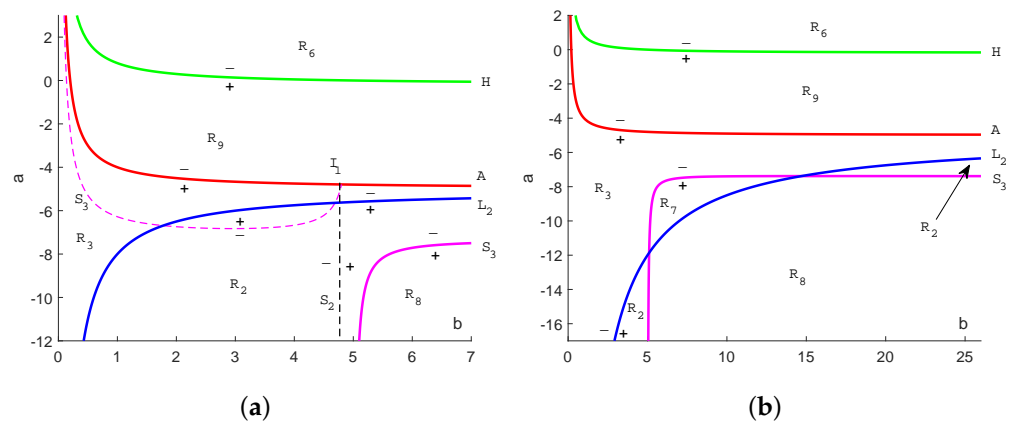


Figure 5. Bifurcation diagrams of the system (3) for $0 < c < 1, d > 0$ and (a) $-c_0d < m < 0$, respectively, (b) $m < -c_0d < 0$.

S_2 is the vertical line $b = \frac{1}{c} - c$, thus, $s_2 < 0$ on the left of S_2 and $s_2 > 0$ on the right of S_2 , for all $c > 0$ arbitrary fixed. If $c = 1$, $s_2 = b$. If $c > 1$, the curve S_2 lies on $b < 0$, thus, it is outside the region of interest. However, the sign of s_2 is important if $c > 1$ as well.

If $c \neq 1$, the curve S_3 has in R two branches asymptotically to the vertical line $b = \frac{1}{c}$ (on the left and right of the line) given by $s_3 = 2b\frac{1-bc}{c}a + (c - \frac{3}{c})b^2 + (\frac{3}{c^2} + c^2)b - \frac{2}{c} = 0$. Notice that $s_3 = \frac{c^2-1}{c} \neq 0$ if $b = \frac{1}{c}$. It follows that $s_3 < 0$ in the region from R that contains $(0,0)$. The sign of s_3 changes when (b, a) crosses a branch of S_3 , as shown in Figures 2–5. Notice that a branch of the curve S_3 may lie on $\alpha < 0$, especially if $c > 1$, and this branch is not taken into account (it is not depicted in Figures 3 and 4) because $P_{2,3}$ do not exist on $\alpha < 0$.

If $c = 1$, then $s_3 = 2(1 - b)(b + ab - 1)$, thus, S_3 has two branches in R as well: one is the vertical line $b = 1$ and the other is the curve A , as shown in Figure 3b. It is clear that $s_3 < 0$ in the region from R that contains $(0,0)$.

If $0 < c < 1$, the curves A, S_2 and S_3 intersect at the same point $I_1 = (b_1, a_1)$, with $b_1 = \frac{1}{c} - c > 0$ and $a_1 = \frac{2c^2-1}{c-c^3}$. If in addition $md > 0$, then $L_1 \cap S_2 = \{I_2\}$, $I_2 = (b_2, a_2)$, where $b_2 = b_1$ and $a_2 = a_1 - \frac{m^2c}{d^2(1-c^2)}$, thus, $a_2 < a_1$. If $md < 0$, then $L_2 \cap S_2 = \{I_2\}$.

Since $m_0 = cm\frac{m^2-d^2\alpha}{d^2}$, $\lambda_4^{P_2} = m - d\sqrt{\alpha}$ and $\lambda_4^{P_3} = m + d\sqrt{\alpha}$, by Theorem 5, the curves $L_1 : \lambda_4^{P_2} = 0$ and $L_2 : \lambda_4^{P_3} = 0$ divide the region R into two disjoint subregions (on the left

and right of L_1 , and the same for L_2), as shown in Figures 2–5. On one subregion P_4 is a saddle, while on the other P_4 is a saddle or an attractor.

The following theorem clarifies the intersection of the bifurcation curves L_1 and S_3 . Since $\lambda_4^{P_2}$ has constant sign on $\alpha > 0$ if $md < 0$, only the case $md > 0$ is needed. We assume further $m > 0$ and $d > 0$. The case $m < 0$ and $d < 0$ is similar.

Theorem 6. Assume $m > 0$ and $d > 0$. The following assertions are true.

- (1) If $0 < c < 1$ and $b > \frac{1}{c}$, the intersection $L_1 \cap S_3$ on $\alpha > 0$ has zero points if $0 < m < dc_0$, one point if $m = dc_0$, respectively, two points if $m > dc_0$, where $c_0 = \frac{c+1}{c\sqrt{2}}\sqrt{1-c^2}$.
- (2) If $0 < c < 1$ and $0 < b \leq \frac{1}{c}$, then either $s_2 < 0$ or $s_3 < 0$ on $\alpha > 0$.
- (3) If $c \geq 1$, the intersection $L_1 \cap S_3$ has a single point on $\alpha > 0$ and $b > 0$.

Proof. Since $\lambda_4^{P_2} = m - d\sqrt{\alpha}$, the curve L_1 is defined only on $\alpha > 0$ and is given by $a = \frac{1}{b} - \frac{1}{c} - \frac{m^2}{bd^2}$, with $b > 0$. The intersection $L_1 \cap S_3$ satisfies $s_3 = 0$ and $\lambda_4^{P_2} = 0$, which lead to an equation in b of the form

$$\left(c - \frac{1}{c}\right)b^2 + \left(\frac{2m^2}{d^2} + \frac{1}{c^2} + c^2 - 2\right)b - \frac{2m^2}{cd^2} = 0. \tag{11}$$

- (1) By $w = b - \frac{1}{c}$, (11) reads $p_0w^2 + p_1w + p_0 = 0$, where $p_0 = c - \frac{1}{c}$ and $p_1 = \frac{2m^2}{d^2} - \frac{1}{c^2} + c^2$. Its roots $w_{1,2}$ satisfy $w_1w_2 = 1$. Thus, $w_1 > 0$ and $w_2 > 0$ iff $w_1 + w_2 > 0$ and $\Delta > 0$ (the discriminant). Since $p_0 < 0$, the inequalities lead to $p_1 > 0$ and $\Delta = (p_1 - 2p_0)(p_1 + 2p_0) > 0$, that is, $p_1 > 0$ and $p_1 + 2p_0 > 0$. However, $p_1 + 2p_0 = 2\left(\frac{m^2}{d^2} - c^2\right) > 0$, where $c_0 = \frac{c+1}{c\sqrt{2}}\sqrt{1-c^2} > 0$, and $m > 0$, lead to $m > dc_0$. Moreover, $p_1 + 2p_0 > 0$ leads to $\frac{2m^2}{d^2} > 2c_0^2 > \frac{1}{c^2} - c^2 > 0$, which, in turn, leads to $p_1 > 0$. Therefore, $w_1 > 0$ and $w_2 > 0$ iff $m > dc_0$. In this case $L_1 \cap S_3 = \{I_3, I_4\}$, where $I_i = (b_i, a_i)$, $a_i = \frac{1}{b_i} - \frac{1}{c} - \frac{m^2}{b_i d^2}$, $i = 3, 4$, respectively, $b_3 = w_1 + \frac{1}{c}$ and $b_4 = w_2 + \frac{1}{c}$. It is clear that $I_3 = I_4$ if $m = dc_0$. If $0 < m < dc_0$ and $p_1 > 0$, then $\Delta < 0$, thus $L_1 \cap S_3$ is the empty set.
- (2) If $0 < b < \frac{1}{c} - c$, then $s_2 < 0$. If $b = \frac{1}{c} - c$, then $s_2 = 0$ and $s_3 = -2c\alpha < 0$ on $\alpha > 0$, while, $s_3 = \frac{c^2-1}{c} < 0$ if $b = \frac{1}{c}$. Let $\frac{1}{c} - c < b < \frac{1}{c}$ and $\alpha > 0$. Then $s_2 > 0$ and

$$s_3 = 2\alpha \frac{bc-1}{c} - \frac{b}{c}s_2(1-c^2) < 0.$$

- (3) Assume $c > 1$. Then, the roots $b_{5,6}$ of (11) satisfy $b_5b_6 < 0$, thus, $b_5 > 0$ and $b_6 < 0$; notice that the discriminant of Equation (11) is positive. It follows that $L_1 \cap S_3 = \{I_5\}$, where $I_5 = (b_5, a_5)$ and $a_5 = \frac{1}{b_5} - \frac{1}{c} - \frac{m^2}{b_5 d^2}$. If $c = 1$, then $L_1 \cap S_3 = \{I_5\}$, where $I_5 = \left(1, -\frac{m^2}{d^2}\right)$.

The theorem is now proved. \square

A similar result can be obtained for the intersection of the curve L_2 with S_3 . Since $\lambda_4^{P_3} = m + d\sqrt{\alpha}$ has constant sign on $\alpha > 0$ if $md > 0$, only the case $md < 0$ is needed. We present the result for $m < 0$ and $d > 0$, while the remaining case $m > 0$ and $d < 0$ can be treated similarly. A proof of the next theorem can be obtained as above.

Theorem 7. Assume $m < 0$ and $d > 0$. The following assertions are true.

- (1) If $0 < c < 1$ and $b > \frac{1}{c}$, the intersection $L_2 \cap S_3$ on $\alpha > 0$ has zero points if $-dc_0 < m < 0$, one point if $m = -dc_0$, respectively, two points if $m < -dc_0 < 0$.
- (2) If $0 < c < 1$ and $0 < b \leq \frac{1}{c}$, then either $s_2 < 0$ or $s_3 < 0$ on $\alpha > 0$.
- (3) If $c \geq 1$, the intersection $L_2 \cap S_3$ has a single point on $\alpha > 0$ and $b > 0$.

Remark 5. For $d > 0$ and $m \in \mathbb{R}$ we obtain:

- (1) If $m > 0$ and $d > 0$, then $\lambda_4^{P_3} = m + d\sqrt{\alpha} > 0$ and $m_0 = cm \frac{\lambda_4^{P_2} \lambda_4^{P_3}}{d^2}$ has the same sign as $\lambda_4^{P_2}$ on $\alpha > 0$, and $m_0 > 0$ if $\alpha \leq 0$. The curves $\{m_0 = 0\}$ and L_1 coincide.
- (2) If $m < 0$ and $d > 0$, then $\lambda_4^{P_2} = m - d\sqrt{\alpha} < 0$ and m_0 has the same sign as $\lambda_4^{P_3}$ on $\alpha > 0$, and $m_0 < 0$ if $\alpha \leq 0$. The curve $\{m_0 = 0\}$ coincides to L_2 in this case.

Remark 6. In the following cases, we will determine the bifurcation diagrams of the system (3) when $m > 0$ and $d > 0$, respectively, $m < 0$ and $d > 0$. One can proceed similarly in other cases.

Case 1. Assume first $0 < c < 1, m > 0$ and $d > 0$. Notice that $\lambda_4^{P_3} > 0$, whenever P_3 exists, and $\{m_0 = 0\}$ coincides to L_1 . Based on Theorem 6, two main bifurcation diagrams arise to describe the system’s dynamics, as shown in Figure 2a,b. The bifurcation curves in the two diagrams are illustrated in Matlab: Figure 2a uses $c = 0.2, m = 1$ and $d = 0.5$, while Figure 2b $c = 0.4, m = 2.7$ and $d = 1$.

Case 2. Assume $c > 1, m > 0$ and $d > 0$. Then S_2 lies on $b < 0$ and $s_2 > 0$ on $b > 0$. By Theorem 6, $L_1 \cap S_3 = \{I_5\}$ in the region $\alpha > 0$ from R . One can show $A \cap S_3 = \emptyset$ on $b > 0$ and $\beta_1 < 0$ in the region R where $\alpha < 0$. As in case 1, $\lambda_4^{P_3} > 0$ on $\alpha > 0$ and $\{m_0 = 0\}$ coincides to L_1 . In particular, if $c = 1$, then $s_2 = b > 0$ and $s_3 = 2(b - 1)\alpha$. Two main bifurcation diagrams emerge in this case, which are depicted in Figure 3a,b. The curves are illustrated for $c = 2, m = 1$ and $d = 0.6$ in Figure 3a, respectively, $c = 1, m = 1$ and $d = 0.6$ in Figure 3b.

Case 3. Assume $c > 1, m < 0$ and $d > 0$. The curve L_2 is given by the same expression as L_1 . The curve $\{m_0 = 0\}$ coincides to L_2 in this case; $\lambda_4^{P_2} < 0$ whenever P_2 exists. Furthermore, $sign(m_0) = sign(\lambda_4^{P_3})$ on $\alpha > 0$ and $m_0 < 0$ if $\alpha \leq 0$, respectively, $\beta_1 < 0$ in the region R where $\alpha < 0$. Using Theorem 7, a bifurcation diagram is presented in Figure 4a. Figure 4b presents a region R_8^1 where P_4 is an attractor, in a typical case $m = -1, d = 0.5$ and $c = 2$. The strip R_8^1 is quite large, it extends to infinity along the horizontal axis when $b > 0$ is large. We denoted by K_1 the curve $\{(b, a), k_1 = 0\}$.

Case 4. Assume $0 < c < 1, m < 0$ and $d > 0$, thus, $\lambda_4^{P_2} < 0$ if $\alpha > 0$. By Theorem 7, two main bifurcation diagrams arise to describe the system’s dynamics, as shown in Figure 5a,b. Figure 5a is illustrated for $c = 0.2, m = -1$ and $d = 0.5$, while Figure 5b for $c = 0.2, m = -3$ and $d = 0.5$.

Remark 7. The type of the equilibria $P_1, P_{2,3}$ and P_4 as they appear in different regions from the above bifurcation diagrams presented in Figures 2–5, are described in Table 1.

Table 1. The type of the equilibria P_1, P_2, P_3 and P_4 on different regions from bifurcation diagrams; s stands for saddle, while a for attractor.

	R_1	R_2	R_3	R_4	R_5	R_6	R_7	R_8	R_9
P_1	s	s	s	s	s	a	s	s	s
P_2	–	s	s	a	a	–	a	s	–
P_3	–	s	s	s	s	–	a	a	–
P_4	a, s	a, s	s	s	a, s	s	s	a, s	s

The different behavior of P_1 as an attractor on the region R_6 is presented in Figure 6, while the two possible states of P_4 as an attractor or saddle are depicted in Figure 7.

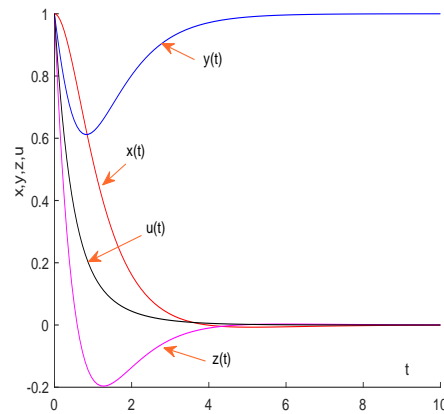


Figure 6. The time series of the four variables around the attractor P_1 in the system (3). The parameters are $a = 1, b = 1, c = 2, m = -1$ and $d = 1$. The starting point of these series is $(1, 1, 1, 1)$.

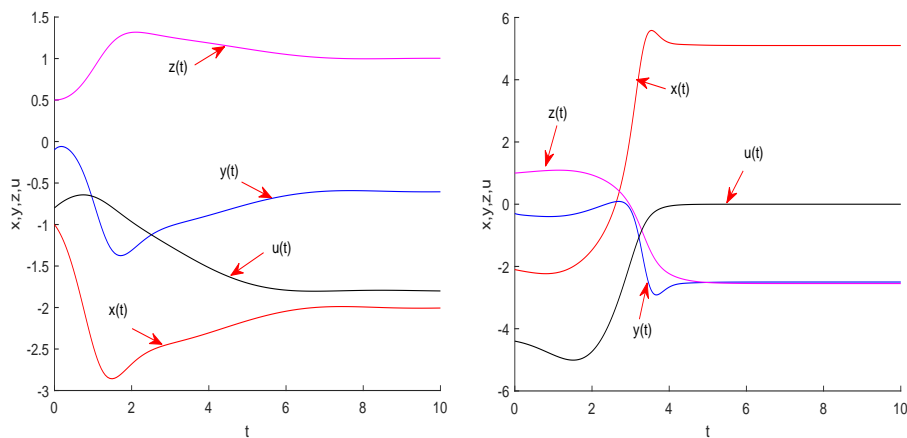


Figure 7. (Left). The time series of the four variables when P_4 is an attractor within the region R_8 . The parameters are $a = -2, b = 5, c = 2, m = -1, d = 0.5$ and $P_4(-2, -0.6, 1, -1.8)$. The starting point of these series is $(-1, -0.1, -0.5, -0.8)$. One may notice that the four series converge correspondingly to the four coordinates of P_4 as t increases, that is, $x(t) \rightarrow -2, y(t) \rightarrow -0.6, z(t) \rightarrow 1$, and $u(t) \rightarrow -1.8$. **(Right).** The time series of the four variables when P_4 is a saddle within the region R_8 . The parameters are $a = -3, b = 10, c = 2, m = -1, d = 0.5$ and $P_4(-2, -0.3, 1, -4.4)$. The starting point of these series is $(-2.1, -0.3, 1, -4.4)$. One may notice that the four series do not converge correspondingly to the four coordinates of P_4 as t increases.

4. Conclusions

An economic model based on differential equations with four variables, the real interest rate, the investment demand, the inflation rate and a control function of the system, has been investigated. The model builds upon a three-dimensional model studied earlier in [14], to which a new variable and equation related to the real interest rate are added. A qualitative analysis has been performed and more bifurcation diagrams were obtained for understanding its local behavior, which undergoes three bifurcations: transcritical, pitchfork and Hopf. Bifurcation diagrams are used to illustrate how the dynamics of the 4D system alters with the increasing value of the parameters m and c . The occurrence of Hopf bifurcation means that the system’s equilibrium points can evolve into predictable economic cycle.

The system (3) proposed in this work has three equilibrium points with economic relevance, P_1, P_3 and P_4 , while the initial system studied in [14], which corresponds to $u = 0$ in (3), has only one steady state with economic relevance, the point P_1 . Thus, the control function u proposed in this work increases the relevance of the initial model. This could lead

to a better understanding of economical prediction for more complex financial phenomena and also explain complex and dynamic behaviour of various economic systems. When the control function is null, we notice that the saving amount variable a is inversely proportional with the fluctuation of the system, meaning the smaller the saving amount is, the bigger the fluctuation of the system is, so the saving amount has to keep a balance because a too small saving amount means chaotic phenomenon and a too large saving amount means a slow economy. When the control function is different from zero, the Routh-Hurwitz criterion is used to study the properties of the asymptotic stability of the economic model with control. This control function can improve the economic vigor and become a necessary condition, in order to make the economy develop well. Numerical simulations are provided using Matlab in order to illustrate the effectiveness of the proposed approaches.

Author Contributions: Conceptualization, G.M.; methodology, G.M.; software, G.M.; validation, G.M., O.B. and A.G.; formal analysis, G.M.; investigation, G.M., O.B. and A.G.; resources, G.M.; data curation, G.M.; writing—original draft preparation, G.M., O.B. and A.G.; writing—review and editing, G.M., O.B. and A.G.; visualization, G.M.; supervision, G.M.; project administration, G.M.; funding acquisition, G.M. All authors have read and agreed to the published version of the manuscript.

Funding: This research was funded by Horizon2020-2017-RISE-777911 project.

Institutional Review Board Statement: Not applicable.

Informed Consent Statement: Not applicable.

Data Availability Statement: Not applicable.

Conflicts of Interest: The authors declare no conflict of interest.

References

1. Angeli, D.; Rishi, A.; Rawlings, J. On average performance and stability of economic model predictive control. *IEEE Trans. Autom. Control* **2011**, *57*, 1615–1626. [[CrossRef](#)]
2. Aizawa, H.; Ikeda, K.; Osawa, M.; Gaspar, J.M. Breaking and sustaining bifurcations in S_N -invariant equidistant economy. *Int. J. Bifurc. Chaos* **2020**, *30*, 2050240. [[CrossRef](#)]
3. Danca, M.F. Coexisting hidden and self-excited attractors in an economic model of integer or fractional order. *Int. J. Bifurc. Chaos* **2021**, *31*, 2150062. [[CrossRef](#)]
4. Guerrini, L. Bifurcation analysis of an economic model. *Int. J. Math. Anal.* **2012**, *6*, 2779–2787.
5. Medio, A.; Pireddu, M.; Zanolin, F. Chaotic dynamics for maps in one and two dimensions: A geometrical method and applications to economics. *Int. J. Bifurc. Chaos* **2009**, *19*, 3283–3309. [[CrossRef](#)]
6. Minsky, H. *Stabilizing an Unstable Economy: A Twentieth Century Fund Report*; Yale University Press: London, UK, 1986.
7. Romer, D. *Advanced Macroeconomics*; McGraw-Hill: New York, NY, USA, 2012.
8. Rigatos, G. *State-Space Approaches for MODELLING and control in Financial Engineering*; Springer: Cham, Switzerland, 2017.
9. Skovranek, T.; Podlubny, I.; Petras, I. Modeling of the national economies in state-space: A fractional calculus approach. *Econ. Model.* **2012**, *29*, 1322–1327. [[CrossRef](#)]
10. Pelgrin, F.; Venditti, A. On the long-run fluctuations of inheritance in two-sector OLG models. *J. Math. Econ.* **2022**, *101*, 102670. [[CrossRef](#)]
11. Ye, R.; Li, X.; Ye, Y.; Zhang, B. DynamicNet: A time-variant ODE network for multi-step wind speed prediction. *Neural Netw.* **2022**, *152*, 118–139. [[CrossRef](#)] [[PubMed](#)]
12. Bai, J.; Wang, X.; Wang, J. An epidemic-economic model for COVID-19. *Math. Biosci. Eng.* **2022**, *19*, 9658–9696. [[CrossRef](#)] [[PubMed](#)]
13. Rigatos, G.; Siano, P.; Ghosh, T.; Sarno, D. A nonlinear optimal control approach to stabilization of a macroeconomic development model. *Quant. Financ. Econ.* **2018**, *2*, 373–387. [[CrossRef](#)]
14. Ma, J.; Chen, Y. Study for the bifurcation topological structure and the global complicated character of a kind of nonlinear finance system. *Appl. Math. Mech.* **2001**, *22*, 1240–1251. [[CrossRef](#)]
15. Chen, W.C. Nonlinear dynamics and chaos in a fractional-order financial system. *Chaos Solitons Fractals* **2008**, *36*, 1305–1314. [[CrossRef](#)]
16. Zhen, W.; Xia, H.; Guodong, S. Analysis of nonlinear dynamics and chaos in a fractional order financial system with time delay. *Comput. Math. Appl.* **2011**, *62*, 1531–1539.
17. Jajarmi, A.; Hajipour, M.; Baleanu, D. New aspects of the adaptive synchronization and hyperchaos suppression of a financial model. *Chaos Solitons Fractals* **2017**, *99*, 285–296. [[CrossRef](#)]

18. Alidousti, J.; Ghahfarokhi, M.M. Stability and bifurcation for time delay fractional predator prey system by incorporating the dispersal of prey. *Appl. Math. Model.* **2019**, *72*, 385–402. [[CrossRef](#)]
19. Alidousti, J. Stability and bifurcation analysis for a fractional prey-predator scavenger model. *Appl. Math. Model.* **2020**, *81*, 342–355. [[CrossRef](#)]
20. Huang, C.; Wang, J.; Chen, X.; Cao, J. Bifurcations in a fractional-order BAM neural network with four different delays. *Neural Netw.* **2021**, *141*, 344–354. [[CrossRef](#)] [[PubMed](#)]
21. Huang, C.; Liu, H.; Chen, X.; Zhang, M.; Ding, L.; Cao, J.; Alsaedi, A. Dynamic optimal control of enhancing feedback treatment for a delayed fractional order predator-prey model. *Phys. A Stat. Mech. Appl.* **2020**, *554*, 124136. [[CrossRef](#)]
22. Xu, C.; Liu, Z.; Liao, M.; Yao, L. Theoretical analysis and computer simulations of a fractional order bank data model incorporating two unequal time delays. *Expert Syst. Appl.* **2022**, *199*, 116859. [[CrossRef](#)]
23. Perko, L. *Differential Equations and Dynamical Systems*, 3rd ed.; Springer: New York, NY, USA, 2001.
24. Kuznetsov, Y.A. *Elements of Applied Bifurcation Theory*, 3rd ed.; Springer: New York, NY, USA, 2004.

Disclaimer/Publisher’s Note: The statements, opinions and data contained in all publications are solely those of the individual author(s) and contributor(s) and not of MDPI and/or the editor(s). MDPI and/or the editor(s) disclaim responsibility for any injury to people or property resulting from any ideas, methods, instructions or products referred to in the content.